Optical and Quantum Electronics (2024) 56:1311
https://doi.org/10.1007/s11082-024-07209-6

Construction of some new traveling wave solutions to the space-time fractional modified equal width equation in modern physics

Fazal Badshah[1] · Kalim U. Tariq[2] · Mustafa Inc[3] · Shahram Rezapour[4] · Abdullah Saad Alsubaie[5] · Sana Nisar[2]

Received: 7 December 2023 / Accepted: 21 June 2024 / Published online: 18 July 2024
© The Author(s) 2024

Abstract
Nonlinear fractional evolution equations are important for determining various complex nonlinear problems that occur in various scientific fields, such as nonlinear optics, molecular biology, quantum mechanics, plasma physics, nonlinear dynamics, water surface waves, elastic media and others. The space-time fractional modified equal width (MEW) equation is investigated in this paper utilizing a variety of solitary wave solutions, with a particular emphasis on their implications for wave propagation characteristics in plasma and optical fibre systems. The fractional-order problem is transformed into an ordinary differential equation using a fractional wave transformation approach. In this article, the polynomial expansion approach and the sardar sub-equation method are successfully used to evaluate the exact solutions of space-time fractional MEW equation. Additionally, in order to graphically represent the physical significance of created solutions, the acquired solutions are shown on contour, 3D and 2D graphs. Based on the results, the employed methods show their efficacy in solving diverse fractional nonlinear evolution equations generated across applied and natural sciences. The findings obtained demonstrate that the two approaches are more effective and suited for resolving various nonlinear fractional differential equations.

Keywords The space-time fractional MEW equation · The polynomial expansion approach · The sardar sub-equation method · Travelling wave solutions · Stability analysis

1 Introduction

From a mathematical perspective, nonlinear phenomena are among the most significant research areas that emerge in many domains of science, including solid-state and plasma physics, fluid mechanics, optical fibres, chemical kinematics and biology. Nonlinear evolution equations (NLEEs) are frequently produced by the mathematical modelling of nonlinear phenomena. To better understand the behaviour of these phenomena, it can be very useful to obtain the NLEE solutions Rezazadeh et al. (2020). The first researchers to explore fractional differential equations (FDEs) are Oldham and Spanier Oldham and Spanier

Extended author information available on the last page of the article

(1974). Currently, fractional differential equations have an important role in a variety of academic disciplines, such as electricity, electronics biological control theory, systems verification, the field of finance, mechanics, engineering, signal analysis, random dynamic systems, plasma therapy physics and quantum systems Sagheer et al. (2019), Abdel-Aty et al. (2020), Kadkhoda and Jafari (2017), Tajadodi et al. (2021)), [7], Zidan et al. (2017), Zidan et al. (2019). The methods we have employed, the polynomial expansion approach and the Sardar sub-equation method, have never been used before in the context of the space-time fractional MEW equation. Previously, the governing model have been investigated by virous analytical approaches including the unified method Rafiq et al. (2022), the expansion method Ali et al. (2022), the improved Bernoulli sub-equation function method Zaman et al. (2023), the Kudryashov method Raslan et al. (2017) and several others.

Over the past few decades, a diverse range of researchers has successfully delved into the exploration of exact solutions and analytical approximations for NLEEs. Notably, various well-established methods have emerged in recent literature (Demirbilek and Mamedov 2023; Rasool et al. 2023; Pandir and Yasmin 2023) and also including the extended trial equation method Nawaz et al. (2017), the Hirota's bilinear form Ma et al. (2018), the extended simplest equation scheme Torvattanabun et al. (2018), the improved F-expansion procedure Bashar and Islam (2020), the Adomian decomposition approach Ikram et al. (2019), the Riccati sub-equation technique Khodadad et al. (2017), the unified method Osman et al. (2018), the advanced auxiliary equation technique Bashar et al. (2022), etc. To obtain analytical solutions for FDEs, a number of reliable approaches have recently been developed. Examples of such techniques include the Kudryashov approach (Seadawy et al. 2017; Lu et al. 2018), the generalized tanh-coth technique (Manafian and Lakestani 2017), the exponential rational function technique (Seadawy and Manafian 2018; Seadawy and El-Rashidy 2018), the simplest equation approach, the modified simple equation approach (Chen and Jiang 2018), the auxiliary equation technique (Khater et al. 2006), the improved F-expansion technique (Seadawy 2018), the first integral approach (Aminikhah et al. 2015) and many others (Alquran 2022; Jaradat and Alquran 2020, 2022; Alquran 2023; Alquran and Al Smadi 2023).

The selected techniques, the polynomial expansion approach and the Sardar sub-equation method, offer several advantages. These methods, being applied to the space-time fractional MEWE for the first time, have yielded several new solutions that can be utilized in various fields. The primary advantages include the ability to derive exact analytical solutions, providing clear insights into the behavior of the equation under different conditions. However, these methods have some limitations. Despite these limitations, once the necessary conditions are met, the methods can be successfully applied to several nonlinear equations, resulting in valuable new solutions.

2 The conformable fractional derivative

In contrast to the integer derivative, the fractional derivative exhibits global association and may provide a more accurate picture of the dynamic functions building processes. Fluid mechanics, applied mathematics, hydrodynamics, quasi-chaotic dynamical systems, system identification, finance, statistics, chaotic dynamical systems, ecology, solid-state biology, optical fibres, electric control theory, and many other topics are among those that can be formulated using fractional calculus. In contrast to conventional calculus, which only considers the current state of the problem, fractional derivatives, which are utilised in the

mathematical modelling of these circumstances, provide a reasonable explanation for the nonlocal nature of these models. The purpose of this special issue is to bring together top academics from a variety of engineering disciplines, including applied mathematicians, and give them a forum to exchange their creative research findings (Jena and Chakraverty 2019; Seadawy et al. 2024; Kırcı et al. 2024; Tariq et al. 2024).

In literature, a variety of fractional derivatives are devised to characterize many crucial physical phenomena, For instance, the modified Riemann-Liouville derivative of Jumarie Jumarie (2006), for Riemann-Liouville derivative (Podlubny 1999), the conformable derivative of Atangana Wu et al. (2020), their Caputo derivative (Almeida 2017) or the Beta-derivative (Gurefe 2020), have been used in many applications in different fields of contemporary science and engineering; fractional-order derivatives provide a more suitable illustration (Bekir et al. 2021). Let $\psi: [0, \infty) \to R$, The conformable derivative fractional ψ of an order β is defined

$$\mathcal{D}_x^{\beta}\psi(x) = \lim_{\varepsilon \to 0} \frac{\psi\left(\varepsilon x^{1-\beta} + x\right) - \psi(x)}{\varepsilon},$$

for each $x > 0$ and $\beta \in (0, 1)$. Additionally, a few characteristics of conformable fractional derivatives are provided

$$\begin{aligned} \mathcal{D}_x^{\beta}(x^{\gamma}) &= \lambda x^{\gamma-\beta}, \forall \gamma \in R, \\ \mathcal{D}_x^{\beta}(\mu(x) + \upsilon(x)) &= \mathcal{D}_x^{\beta}\mu(x) + \mathcal{D}_x^{\beta}\upsilon(x), \\ \mathcal{D}_x^{\beta}(\mu o \upsilon)(x) &= x^{1-\beta}\upsilon(x^{\beta-1})\upsilon'(t)\mathcal{D}_x^{\beta}(\mu(x))|_{x=\mu(x)}. \end{aligned}$$

3 The governing model

The fractional-order MEW equation, a nonlinear wave equation renowned for its relevance in describing wave phenomena in shallow water and plasmas, presents solutions featuring a distinctive interplay of positive and negative amplitudes. One intriguing characteristic of these solutions is the uniformity in their width. This peculiar aspect signifies that, while the amplitude may vary, the spatial extent of the waves remains unaltered. The space-time fractional MEW equation (Hosseini and Ayati 2016) takes the following format:

$$D_t^{\alpha}\mathcal{L}(x,t) + \epsilon \mathrm{D}_x^{\alpha}\mathcal{L}^3(x,t) - \mu \mathrm{D}_{xxt}^{3\alpha}\mathcal{L}(x,t) = 0, \tag{1}$$

where the actual parameters are μ and ϵ respectively. In the given scenario, x and t denote space and time coordinates, respectively. The function $\mathcal{L}(x,t)$ represents the amplitude of a wave. The space-time fractional MEW equation can lead to solutions that are either real-valued or complex-valued functions, depending on the specific parameters and initial or boundary conditions of the problem. The notation D_t^{α} symbolizes the conformable fractional derivative of $\mathcal{L}$ concerning time t with an order α. In fluid dynamics, $\mathcal{L}$ shows how the water surface moves up and down due to long waves and in plasma physics, it represents the negative electric potential. It's interesting how $\mathcal{L}$ can mean different things in different areas of science, like waves in water or electrical properties in plasmas. In recent years, scientists have been working on solving (1): Korkmaz (2017) found solutions using trigonometric and hyperbolic functions, Raslan et al. (2017) discovered new solutions with a modified method and Shallal et al. (2020) used a generalized expansion method. These

findings help us better understand the MEW equation and how different mathematical methods can be applied to study it.

The space-time fractional MEW equation is a type of partial differential equation that includes fractional derivatives with respect to both space and time variables and it is modified to incorporate the equal width property. This equation has applications in various fields, particularly in the study of nonlinear waves and solitons. The MEW equation describes the evolution of nonlinear waves with fractional order derivatives. It is used to model the behavior of waves in different media, such as fluids, plasmas, or optical fibers, where the equal width property is relevant. This model can support soliton solutions, which are stable, localized, and self-reinforcing wave packets. Understanding the dynamics of solitons is crucial in fields like optics, where solitons play a role in signal transmission and information processing (Seadawy et al. 2021; Zafar 2019). Fractional differential equations, including the space-time fractional MEW equation, can be applied to model phenomena in biology, such as the spread of diseases or the diffusion of substances in biological tissues. The fractional order helps capture the memory and hereditary properties often present in biological systems. The governing model may find applications in plasma physics, where the behavior of charged particles in a plasma is modeled. Understanding the dynamics of plasma waves is crucial in areas like fusion research and space physics. Fractional differential equations can be used to model the transport properties of materials, including the diffusion of substances through porous media or the propagation of heat in materials with fractional properties (Raslan et al. 2017). The nonlinear structure can be relevant in the study of optical pulse propagation in fiber optics. Understanding how optical signals evolve in optical fibers is important for designing efficient and robust communication systems. This structure may also be applied to model the dynamics of waves and currents in geophysical fluids, such as ocean waves or atmospheric phenomena. The fractional derivatives help to capture the complex nature of these fluid systems Tariq et al. (2018).

The goal of this article is to explore novel and broad-spectrum soliton solutions for the time-fractional MEW equation. This investigation is conducted by employing the polynomial expansion approach and the Sardar sub-equation method. Furthermore, the article aims to analyze the dynamic behavior of these analytical solutions. The utilization of these mathematical methods provides a comprehensive exploration of soliton solutions and contributes to a deeper understanding of the dynamic characteristics described by the nonlinear model under consideration.

The remainder of the article is structured as follows: The Sardar sub-equation approach and the polynomial expansion approach is described in Sect. 2. The conformable derivative is used in Sect. 3 to produce a variety of new travelling wave solutions and stability analysis in Sect. 4. The graphical depictions of the solutions are elaborated in Sect. 5, while the conclusion is outlined in Sect. 6.

4 Methodology

Consider the nonlinear fractional differential equation shown below to demonstrate the fundamental concept of our approach

$$G\Big(\mathcal{L}, D_t^{\alpha_1}\mathcal{L}, D_x^{2\alpha_1}\mathcal{L}, D_{tt}^{2\alpha_2}\mathcal{L}, D_{xx}^{2\alpha_2}\mathcal{L}, D_t^{\alpha_1}D_t^{\alpha_2}\mathcal{L}, \dots\Big), 0 < \alpha_1, \alpha_2 < 1. \tag{2}$$

Employing the fractional complex transformation

$$\mathcal{L}(x,t) = \mathcal{L}(\mathfrak{V}),\ \mathfrak{V} = \frac{k}{(\alpha_2+1)\Pi}x^{\alpha} - \frac{c}{(\alpha_1+1)\Pi}t^{\alpha} - x_0, \tag{3}$$

reduces (2) into an integer order nonlinear ordinary differential equations as follows, where k and c are nonzero constants, x_0 is an arbitrary constant and α_1 and α_2 are fractional orders.

$$H(\mathcal{L}, \mathcal{L}', \mathcal{L}'', \dots) = 0, \tag{4}$$

where the derivatives are based on $\mathfrak{V}$.

4.1 The modified Sardar sub-equation approach

The solutions to Eq. (4) are viewed as a finite series, it is assumed

$$\mathcal{L}(\mathfrak{V}) = W_0 + \sum_{b=1}^{N} W_b \mathcal{L}^b(\mathfrak{V}),\ W_N \neq 0. \tag{5}$$

We give the integer value of N, which balances the greatest power nonlinear and highest derivative terms.

The following nonlinear ordinary equation can be resolved by the function $\mathcal{L}(\mathfrak{V})$

$$\mathcal{L}'(\mathfrak{V})^2 = \psi_2 \mathcal{L}(\mathfrak{V})^4 + \psi_1 \mathcal{L}(\mathfrak{V})^2 + \psi_0. \tag{6}$$

Additionally, the following are the general solutions to Eq. (6)

Step 1. If $\psi_0 = 0,\ \psi_1 > 0$ and $\psi_2 \neq 0$, we have

$$\mathcal{L}_1(\mathfrak{V}) = \pm \text{Sech}\sqrt{-\frac{\psi_1}{\psi_2}}\left(\sqrt{\psi_1}(\mathfrak{V}+\eta)\right),$$

$$\mathcal{L}_2(\mathfrak{V}) = \pm \text{Csch}\sqrt{-\frac{\psi_1}{\psi_2}}\left(\sqrt{\psi_1}(\mathfrak{V}+\eta)\right).$$

Step 2. If $\psi_0 = 0, \psi_1 > 0$ and $\psi_2 = 4f_1 f_2$, we have

$$\mathcal{L}_3(\mathfrak{V}) = \pm \frac{4f_1\sqrt{\psi_1}}{\left(4f_1^2 - \psi_2\right)\sinh\left(\sqrt{\psi_1}(\mathfrak{V}+\eta)\right) + \left(4f_1^2 - \psi_2\right)\cosh\left(\sqrt{\psi_1}(\mathfrak{V}+\eta)\right)}.$$

Step 3. If $\psi_0 = \frac{\psi_1^2}{4\psi_2},\ \psi_1 < 0$ and $\psi_2 > 0$, we have

$$\mathcal{L}_4(\mathfrak{V}) = \pm\sqrt{-\frac{\psi_1}{2\psi_2}}\tanh\left(\sqrt{-\frac{\psi_1}{2}}(\mathfrak{V}+\eta)\right),$$

$$\mathcal{L}_5(\mathfrak{V}) = \pm\sqrt{-\frac{\psi_1}{2\psi_2}}\coth\left(\sqrt{-\frac{\psi_1}{2}}(\mathfrak{V}+\eta)\right),$$

$$\mathcal{L}_6(\mathfrak{V}) = \pm\sqrt{-\frac{\psi_1}{2\psi_2}}\left(\tanh\left(\sqrt{-\frac{\psi_1}{2}}(\mathfrak{V}+\eta)\right) + i\,\mathrm{sech}\left(\sqrt{-2\psi_1}(\mathfrak{V}+\eta)\right)\right),$$

$$\mathcal{L}_7(\mathfrak{V}) = \pm\sqrt{-\frac{\psi_1}{8\psi_2}}\left(\tanh\left(\sqrt{-\frac{\psi_1}{2}}(\mathfrak{V}+\eta)\right) + \coth\left(\sqrt{-\frac{\psi_1}{8}}(\mathfrak{V}+\eta)\right)\right),$$

$$\mathcal{L}_8(\mathfrak{V}) = \pm\frac{\sqrt{-\frac{\psi_1}{2\psi_2}}\cosh\left(\sqrt{-2\psi_1}(\mathfrak{V}+\eta)\right)}{\sinh\left(\sqrt{-2\psi_1}(\mathfrak{V}+\eta)\right)+i}.$$

Step 4. If $\psi_0 = 0,\ \psi_1 < 0,$ and $\psi_2 \neq 0$, we have

$$\mathcal{L}_9(\mathfrak{V}) = \pm\sqrt{-\frac{\psi_1}{\psi_2}}\sec\left(\sqrt{-\psi_1}(\mathfrak{V}+\eta)\right),$$

$$\mathcal{L}_{10}(\mathfrak{V}) = \pm\sqrt{-\frac{\psi_1}{\psi_2}}\csc\left(\sqrt{-\psi_1}(\mathfrak{V}+\eta)\right).$$

Step 5. If $\psi_0 = \frac{\psi_1^2}{4\psi_2},\ \psi_1 > 0$ *and* $\psi_2 > 0$ and $G_1^2 - G_2^2 > 0$, we have

$$\mathcal{L}_{11}(\mathfrak{V}) = \pm\sqrt{\frac{\psi_1}{2\psi_2}}\tan\left(\sqrt{\frac{\psi_1}{2}}(\mathfrak{V}+\eta)\right),$$

$$\mathcal{L}_{12}(\mathfrak{V}) = \pm\sqrt{\frac{\psi_1}{2\psi_2}}\cot\left(\sqrt{\frac{\psi_1}{2}}(\mathfrak{V}+\eta)\right),$$

$$\mathcal{L}_{13}(\mathfrak{V}) = \pm\sqrt{\frac{\psi_1}{2\psi_2}}\left(\tan\left(\sqrt{2\psi_1}(\mathfrak{V}+\eta)\right) + \sec\left(\sqrt{2\psi_1}(\mathfrak{V}+\eta)\right)\right),$$

$$\mathcal{L}_{14}(\tau) = \pm\sqrt{\frac{\psi_1}{8\psi_2}}\left(\tan\left(\sqrt{\frac{\psi_1}{8}}(\mathfrak{V}+\eta)\right) - \cot\left(\sqrt{\frac{\psi_1}{8}}(\mathfrak{V}+\eta)\right)\right),$$

$$\mathcal{L}_{15}(\mathfrak{V}) = \pm\frac{\sqrt{\frac{\psi_1}{2\psi_2}}\left(\sqrt{G_1^2 - G_2^2} - e_1\cos\left(\sqrt{2\psi_1}(\mathfrak{V}+\eta)\right)\right)}{G_2 + e_1\sin\left(\sqrt{2\psi_1}(\mathfrak{V}+\eta)\right)},$$

$$\mathcal{L}_{16}(\mathfrak{V}) = \pm\frac{\sqrt{\frac{\psi_1}{2\psi_2}}\cos\left(\sqrt{2\psi_1}(\mathfrak{V}+\eta)\right)}{\sin\left(\sqrt{2\psi_1}(\mathfrak{V}+\eta)\right)-1}.$$

Step 6. If $\psi_0 = 0,\ \psi_1 > 0$, we have

$$\mathcal{L}_{17}(\mathfrak{V}) = \pm\frac{4\psi_1 e^{\sqrt{\psi_1}(\mathfrak{V}+\eta)}}{e^{2\sqrt{\psi_1}(\mathfrak{V}+\eta)} - 4\psi_1\psi_2},$$
$$\mathcal{L}_{18}(\mathfrak{V}) = \pm\frac{4\psi_1 e^{\sqrt{\psi_1}(\mathfrak{V}+\eta)}}{1 - 4\psi_1\psi_2 e^{2\sqrt{\psi_1}(\mathfrak{V}+\eta)}}.$$

Step 7. If $\psi_0 = 0,\ \psi_1 = 0$ *and* $\psi_2 > 0$, we have

$$\mathcal{L}_{19}(\mathfrak{V}) = \frac{1}{\sqrt{\psi_2}(\mathfrak{V}+\eta)},$$
$$\mathcal{L}_{20}(\mathfrak{V}) = \pm\frac{i}{\sqrt{\psi_2}(\mathfrak{V}+\eta)}.$$

4.2 The polynomial expansion technique

The major steps in the procedure are briefly summarized in the section below:

Step 1: The solution to Eq. (4) can be stated as

$$\mathcal{L}(\mathfrak{V}) = \sum_{i=1}^{N} n_i \psi(\mathfrak{V})^{-i} + \sum_{i=1}^{N} m_i \psi(\mathfrak{V})^{i} + m_0, \tag{7}$$

where N indicates a real variable and m_i, n_i are the unknowns, additionally, $\psi(\mathfrak{V})$ fulfils

$$\psi'(\mathfrak{V}) = \nu\psi(\mathfrak{V}) + \Pi + \psi(\mathfrak{V})^2, \tag{8}$$

a real constant is represented by the sign $\mathfrak{V}$. According on the given variables, the equation displayed above has a variety of solutions.

Case I. If $\nu = 0,\ \Pi = 0$, the result is eventually determined as

$$\psi(\mathfrak{V}) = -\frac{1}{\mathfrak{V}}.$$

Case II. If $\nu \neq 0,\ \Pi = 0$, the result is eventually determined as

$$\psi(\mathfrak{V}) = -\frac{\nu}{A_0 e^{-\nu\mathfrak{V}} - 1},$$

where A_0 is a integration constant.

Case III. If $\nu = 0,\ \Pi \neq 0,\ \Pi > 0$, the result is eventually determined as

$$\psi(\mathfrak{V}) = \sqrt{\Pi}\tan\left(\sqrt{\Pi}\mathfrak{V}\right),$$
$$\psi(\mathfrak{V}) = -\sqrt{-\Pi}\cot\left(\sqrt{\Pi}\mathfrak{V}\right).$$

Case IV. If $\nu = 0,\ \Pi \neq 0,\ \Pi < 0$, the result is eventually determined as

$$\psi(\mathfrak{V}) = -\sqrt{-\Pi}\tanh\left(\sqrt{-\Pi}\mathfrak{V}\right),$$
$$\psi(\mathfrak{V}) = \sqrt{-\Pi}\coth\left(\sqrt{-\Pi}\mathfrak{V}\right).$$

Case V. If $\Pi \neq 0, \quad \nu \neq 0$, the result is eventually determined as

$$\psi(\mho) = \frac{\psi_1 - A_1\psi_2 e^{\mho(\psi_1-\Theta_2)}}{1 - A_1 e^{\mho(\psi_1-\psi_2)}},$$

a constant of integration is A_1. ψ_1 and ψ_2 is one of the roots of the equation $\psi^2 + \nu\psi + \Pi$ i.e.

$$\psi_1 = \frac{-\nu + \sqrt{\nu^2 - 4\Pi}}{2}, \qquad \psi_2 = \frac{-\nu - \sqrt{\nu^2 - 4\Pi}}{2}.$$

Step 2: By applying Eqs. (7) and (8) to Eq. (4) and, if all of them were set to zero, we would obtain several mathematical equations by accumulating the same value of $\psi(\mho)$.

Step 3: As a result, in the last stage, one assesses the whole set of equations by combining the quantities obtained with the Eq. (7) and to the Eq. (8) response. This is necessary to properly obtain Eq. (1) accurate wave solutions.

5 Mathematical analysis

The following integer order nonlinear ordinary differential equation is created by transforming Eq. (1) using the fractional complex transformation Eq. (8)

$$-cg' + \varepsilon k(g^3)' + \mu ck^2 g''' = 0, \tag{9}$$

the result of once integrating Eq. (9) with respect to η

$$-cg + \varepsilon k g^3 + \mu ck^2 g'' = 0, \tag{10}$$

here,the integrating constant is considered as zero.

5.1 Applications of the modified sardar subequation technique

g'' and g^3 are balanced in Eq. (10), which results in $N = 1$. When $N = 1$, the solution to Eq. (5) accepts the form

$$\mathcal{L}(\mho) = W_0 + W_1\mathcal{L}(\mho), \tag{11}$$

the following classes of solutions can be obtained by plugging Eq. (16), its second derivative, together with Eq. (6), into Eq. (10).

$$\begin{aligned} W_0^3 \epsilon \mathrm{k} - cW_0 &= 0, \\ -cW_1 + W_1\psi_1\mu \mathrm{ck}^2 + 3W_0^2 W_1 \epsilon \mathrm{k} &= 0, \\ 3W_0 W_1^2 \epsilon \mathrm{k} &= 0, \\ 2W_1\psi_2\mu \mathrm{ck}^2 + W_1^3 \epsilon \mathrm{k} &= 0. \end{aligned}$$

Family I

$$W_0 = 0,\ W_1 = -\frac{i\sqrt{2}\sqrt{\psi_2}\mu \mathrm{ck}}{\sqrt{\epsilon \mathrm{k}}},\ c = \psi_1 \mu \mathrm{ck}^2.$$

Case I: If $\psi_0 = 0,\ \psi_1 > 0$ and $\psi_2 \neq 0$, we have

$$\mathcal{L}_1(x,t) = -\frac{i\sqrt{2}\mathrm{Sech}\sqrt{\psi_1}\sqrt{\psi_2}\mu \mathrm{ck}(\mho + \eta)\left(\pm\sqrt{-\frac{\psi_1}{\psi_2}}\right)}{\sqrt{\epsilon \mathrm{k}}}, \tag{12}$$

$$\mathcal{L}_2(x,t) = -\frac{i\sqrt{2}\mathrm{Csch}\sqrt{\psi_1}\sqrt{\psi_2}\mu \mathrm{ck}(\mho + \eta)\left(\pm\sqrt{-\frac{\psi_1}{\psi_2}}\right)}{\sqrt{\epsilon \mathrm{k}}}. \tag{13}$$

Case II: If $\psi_0 = 0, \psi_1 > 0$ and $\psi_2 = 4f_1 f_2$, we have

$$\mathcal{L}_3(x,t) = -\frac{i\sqrt{2}\sqrt{\psi_2}\mu \mathrm{ck}\left(\pm\frac{4f_1\sqrt{\psi_1}}{\left(4f_1^2-\psi_2\right)\sinh\left(\sqrt{\psi_1}(\mho+\eta)\right)+\left(4f_1^2-\psi_2\right)\cosh\left(\sqrt{\psi_1}(\mho+\eta)\right)}\right)}{\sqrt{\epsilon \mathrm{k}}}. \tag{14}$$

Case III: If $\psi_0 = \frac{\psi_1^2}{4\psi_2},\ \psi_1 < 0$ and $\psi_2 > 0$, we have

$$\mathcal{L}_4(x,t) = -\frac{i\sqrt{2}\sqrt{\psi_2}\mu \mathrm{ck}\left(\pm\frac{\sqrt{-\frac{\psi_1}{\psi_2}}}{\sqrt{2}}\right)\tanh\left(\frac{\sqrt{-\psi_1}(\mho+\eta)}{\sqrt{2}}\right)}{\sqrt{\epsilon \mathrm{k}}}, \tag{15}$$

$$\mathcal{L}_5(x,t) = -\frac{i\sqrt{2}\sqrt{y_2}\mu \mathrm{ck}\left(\pm\frac{\sqrt{-\frac{\psi_1}{\psi_2}}}{\sqrt{2}}\right)\coth\left(\frac{\sqrt{-\psi_1}(\mho+\eta)}{\sqrt{2}}\right)}{\sqrt{\epsilon \mathrm{k}}}, \tag{16}$$

$$\mathcal{L}_6(x,t) = -\frac{i\sqrt{2}\sqrt{\psi_2}\mu \mathrm{ck}\left(\pm\frac{\sqrt{-\frac{\psi_1}{\psi_2}}}{\sqrt{2}}\right)\left(\tanh\left(\frac{\sqrt{-\psi_1}(\mho+\eta)}{\sqrt{2}}\right)+i\mathrm{sech}\left(\sqrt{2}\sqrt{-\psi_1}(\mho+\eta)\right)\right)}{\sqrt{\epsilon \mathrm{k}}}, \tag{17}$$

$$\mathcal{L}_7(x,t) = -\frac{i\sqrt{2}\sqrt{\psi_2}\mu \mathrm{ck}\left(\pm\frac{\sqrt{-\frac{\psi_1}{\psi_2}}}{2\sqrt{2}}\right)\left(\tanh\left(\frac{\sqrt{-\psi_1}(\mho+\eta)}{\sqrt{2}}\right)+\coth\left(\frac{\sqrt{-\psi_1}(\mho+\eta)}{2\sqrt{2}}\right)\right)}{\sqrt{\epsilon \mathrm{k}}}, \tag{18}$$

$$\mathcal{L}_8(x,t) = -\frac{i\sqrt{2}\sqrt{\psi_2}\mu \mathrm{ck}\left(\pm\frac{\sqrt{-\frac{\psi_1}{\psi_2}}}{\sqrt{2}}\right)\cosh\left(\sqrt{2}\sqrt{-\psi_1}(\mathfrak{O}+\eta)\right)}{\sqrt{\epsilon \mathrm{k}}\left(\sinh\left(\sqrt{2}\sqrt{-\psi_1}(\mathfrak{O}+\eta)\right)+i\right)}. \tag{19}$$

Case IV: If $\psi_0 = 0,\ \psi_1 < 0,$ and $\psi_2 \neq 0$, we have

$$\mathcal{L}_9(x,t) = -\frac{i\sqrt{2}\sqrt{\psi_2}\mu \mathrm{ck}\left(\pm\sqrt{-\frac{\psi_1}{\psi_2}}\right)\sec\left(\sqrt{-\psi_1}(\mathfrak{O}+\eta)\right)}{\sqrt{\epsilon \mathrm{k}}}, \tag{20}$$

$$\mathcal{L}_{10}(x,t) = -\frac{i\sqrt{2}\sqrt{\psi_2}\mu \mathrm{ck}\left(\pm\sqrt{-\frac{\psi_1}{\psi_2}}\right)\csc\left(\sqrt{-\psi_1}(\mathfrak{O}+\eta)\right)}{\sqrt{\epsilon \mathrm{k}}}. \tag{21}$$

Case V: If $\psi_0 = \frac{\psi_1^2}{4\psi_2},\ \psi_1 > 0$ *and* $\psi_2 > 0$ and $G_1^2 - G_2^2 > 0$, we have

$$\mathcal{L}_{11}(x,t) = -\frac{i\sqrt{2}\sqrt{\psi_2}\mu \mathrm{ck}\left(\pm\frac{\sqrt{-\frac{\psi_1}{\psi_2}}}{\sqrt{2}}\right)\tan\left(\frac{\sqrt{\psi_1}(\mathfrak{O}+\eta)}{\sqrt{2}}\right)}{\sqrt{\epsilon \mathrm{k}}}, \tag{22}$$

$$\mathcal{L}_{12}(x,t) = -\frac{i\sqrt{2}\sqrt{\psi_2}\mu \mathrm{ck}\left(\pm\frac{\sqrt{-\frac{\psi_1}{\psi_2}}}{\sqrt{2}}\right)\cot\left(\frac{\sqrt{\psi_1}(\mathfrak{O}+\eta)}{\sqrt{2}}\right)}{\sqrt{\epsilon \mathrm{k}}}, \tag{23}$$

$$\mathcal{L}_{13}(x,t) = -\frac{i\sqrt{2}\sqrt{\psi_2}\mu \mathrm{ck}\left(\pm\frac{\sqrt{\frac{\psi_1}{\psi_2}}}{\sqrt{2}}\right)\left(\tan\left(\sqrt{2}\sqrt{\psi_1}(\mathfrak{O}+\eta)\right)+\sec\left(\sqrt{2}\sqrt{\psi_1}(\mathfrak{O}+\eta)\right)\right)}{\sqrt{\epsilon \mathrm{k}}}, \tag{24}$$

$$\mathcal{L}_{14}(x,t) = -\frac{i\sqrt{2}\sqrt{\psi_2}\mu \mathrm{ck}\left(\pm\frac{\sqrt{\frac{\psi_1}{\psi_2}}}{2\sqrt{2}}\right)\left(\tan\left(\frac{\sqrt{\psi_1}(\mathfrak{O}+\eta)}{2\sqrt{2}}\right)-\cot\left(\frac{\sqrt{\psi_1}(\mathfrak{O}+\eta)}{2\sqrt{2}}\right)\right)}{\sqrt{\epsilon \mathrm{k}}}, \tag{25}$$

$$\mathcal{L}_{15}(x,t) = -\frac{i\sqrt{2}\sqrt{\psi_2}\mu \mathrm{ck}\left(\pm\frac{\sqrt{\frac{\psi_1}{\psi_2}}}{\sqrt{2}}\right)\left(\sqrt{G_1^2-G_2^2}-e_1\cos\left(\sqrt{2}\sqrt{\psi_1}(\mathfrak{O}+\eta)\right)\right)}{\sqrt{\epsilon \mathrm{k}}\left(G_2+e_1\sin\left(\sqrt{2}\sqrt{\psi_1}(\mathfrak{O}+\eta)\right)\right)}, \tag{26}$$

$$\mathcal{L}_{16}(x,t) = -\frac{i\sqrt{2}\sqrt{\psi_2}\mu \mathrm{ck}\left(\pm\frac{\sqrt{\frac{\psi_1}{\psi_2}}}{\sqrt{2}}\right)\cos\left(\sqrt{2}\sqrt{\psi_1}(\mho+\eta)\right)}{\sqrt{\epsilon \mathrm{k}}\left(\sin\left(\sqrt{2}\sqrt{\psi_1}(\mho+\eta)\right)-1\right)}. \tag{27}$$

Case VI: If $\psi_0 = 0,\ \psi_1 > 0$, we have

$$\mathcal{L}_{17}(x,t) = -\frac{i\sqrt{2}\sqrt{\psi_2}\mu \mathrm{ck}\left(\pm\frac{4\psi_1 e^{\sqrt{\psi_1}(\mho+\eta)}}{e^{2\sqrt{\psi_1}(\mho+\eta)}-4\psi_1\psi_2}\right)}{\sqrt{\epsilon \mathrm{k}}}, \tag{28}$$

$$\mathcal{L}_{18}(x,t) = -\frac{i\sqrt{2}\sqrt{\psi_2}\mu \mathrm{ck}\left(\pm\frac{4\psi_1 e^{\sqrt{\psi_1}(\mho+\eta)}}{1-4\psi_1\psi_2 e^{2\sqrt{\psi_1}(\mho+\eta)}}\right)}{\sqrt{\epsilon \mathrm{k}}}. \tag{29}$$

Case VII: If $\psi_0 = 0,\ \psi_1 = 0$ *and* $\psi_2 > 0$, we have

$$\mathcal{L}_{19}(x,t) = -\frac{i\sqrt{2}\sqrt{\psi_2}\mu \mathrm{ck}\left(\pm\frac{1}{\sqrt{\psi_2}(\mho+\eta)}\right)}{\sqrt{\epsilon \mathrm{k}}}, \tag{30}$$

$$\mathcal{L}_{20}(x,t) = -\frac{i\sqrt{2}\sqrt{\psi_2}\mu \mathrm{ck}\left(\pm\frac{i}{\sqrt{\psi_2}(\mho+\eta)}\right)}{\sqrt{\epsilon \mathrm{k}}}, \tag{31}$$

where $\mho = \frac{k}{(\alpha+1)\Pi}x^{\alpha} - \frac{c}{(\alpha+1)\Pi}t^{\alpha} - x_0$.

Family II:

$$W_0 = 0,\ W_1 = \frac{i\sqrt{2}\sqrt{\psi_2}\mu \mathrm{ck}}{\sqrt{\epsilon \mathrm{k}}},\ W_2 = 0,\ c = \psi_1 \mu \mathrm{ck}^2.$$

Case I: If $\psi_0 = 0,\ \psi_1 > 0$ and $\psi_2 \neq 0$, we have

$$\mathcal{L}_{21}(x,t) = \frac{i\sqrt{2}\mathrm{Sech}\sqrt{\psi_1}\sqrt{\psi_2}\mu \mathrm{ck}(\mho+\eta)\left(\pm\sqrt{-\frac{\psi_1}{\psi_2}}\right)}{\sqrt{\epsilon \mathrm{k}}}, \tag{32}$$

$$\mathcal{L}_{22}(x,t) = \frac{i\sqrt{2}\mathrm{Csch}\sqrt{\psi_1}\sqrt{\psi_2}\mu \mathrm{ck}(\mho+\eta)\left(\pm\sqrt{-\frac{\psi_1}{\psi_2}}\right)}{\sqrt{\epsilon \mathrm{k}}}. \tag{33}$$

Case II: If $\psi_0 = 0, \psi_1 > 0$ and $\psi_2 = 4f_1 f_2$, we have

$$\mathcal{L}_{23}(x,t)=\frac{i\sqrt{2}\sqrt{\psi_2}\mu\mathrm{ck}\left(\pm\frac{4f_1\sqrt{\psi_1}}{\left(4f_1^2-\psi_2\right)\sinh\left(\sqrt{\psi_1}(\mathfrak{O}+\eta)\right)+\left(4f_1^2-\psi_2\right)\cosh\left(\sqrt{\psi_1}(\mathfrak{O}+\eta)\right)}\right)}{\sqrt{\epsilon\mathrm{k}}}. \tag{34}$$

Case III: If $\psi_0=\frac{\psi_1^2}{4\psi_2}$, $\psi_1<0$ and $\psi_2>0$, we have

$$\mathcal{L}_{24}(x,t)=\frac{i\sqrt{2}\sqrt{\psi_2}\mu\mathrm{ck}\left(\pm\frac{\sqrt{-\frac{\psi_1}{\psi_2}}}{\sqrt{2}}\right)\tanh\left(\frac{\sqrt{-\psi_1}(\mathfrak{O}+\eta)}{\sqrt{2}}\right)}{\sqrt{\epsilon\mathrm{k}}}, \tag{35}$$

$$\mathcal{L}_{25}(x,t)=\frac{i\sqrt{2}\sqrt{y_2}\mu\mathrm{ck}\left(\pm\frac{\sqrt{-\frac{\psi_1}{\psi_2}}}{\sqrt{2}}\right)\coth\left(\frac{\sqrt{-\psi_1}(\mathfrak{O}+\eta)}{\sqrt{2}}\right)}{\sqrt{\epsilon\mathrm{k}}}, \tag{36}$$

$$\mathcal{L}_{26}(x,t)=\frac{i\sqrt{2}\sqrt{\psi_2}\mu\mathrm{ck}\left(\pm\frac{\sqrt{-\frac{\psi_1}{\psi_2}}}{\sqrt{2}}\right)\left(\tanh\left(\frac{\sqrt{-\psi_1}(\mathfrak{O}+\eta)}{\sqrt{2}}\right)+i\mathrm{sech}\left(\sqrt{2}\sqrt{-\psi_1}(\mathfrak{O}+\eta)\right)\right)}{\sqrt{\epsilon\mathrm{k}}}, \tag{37}$$

$$\mathcal{L}_{27}(x,t)=\frac{i\sqrt{2}\sqrt{\psi_2}\mu\mathrm{ck}\left(\pm\frac{\sqrt{-\frac{\psi_1}{\psi_2}}}{2\sqrt{2}}\right)\left(\tanh\left(\frac{\sqrt{-\psi_1}(\mathfrak{O}+\eta)}{\sqrt{2}}\right)+\coth\left(\frac{\sqrt{-\psi_1}(\mathfrak{O}+\eta)}{2\sqrt{2}}\right)\right)}{\sqrt{\epsilon\mathrm{k}}}, \tag{38}$$

$$\mathcal{L}_{28}(x,t)=\frac{i\sqrt{2}\sqrt{\psi_2}\mu\mathrm{ck}\left(\pm\frac{\sqrt{-\frac{\psi_1}{\psi_2}}}{\sqrt{2}}\right)\cosh\left(\sqrt{2}\sqrt{-\psi_1}(\mathfrak{O}+\eta)\right)}{\sqrt{\epsilon\mathrm{k}}\left(\sinh\left(\sqrt{2}\sqrt{-\psi_1}(\mathfrak{O}+\eta)\right)+i\right)}. \tag{39}$$

Case IV: If $\psi_0=0,\ \psi_1<0,$ and $\psi_2\neq 0$, we have

$$\mathcal{L}_{29}(x,t)=\frac{i\sqrt{2}\sqrt{\psi_2}\mu\mathrm{ck}\left(\pm\sqrt{-\frac{\psi_1}{\psi_2}}\right)\sec\left(\sqrt{-\psi_1}(\mathfrak{O}+\eta)\right)}{\sqrt{\epsilon\mathrm{k}}}, \tag{40}$$

$$\mathcal{L}_{30}(x,t)=\frac{i\sqrt{2}\sqrt{\psi_2}\mu\mathrm{ck}\left(\pm\sqrt{-\frac{\psi_1}{\psi_2}}\right)\csc\left(\sqrt{-\psi_1}(\mathfrak{O}+\eta)\right)}{\sqrt{\epsilon\mathrm{k}}}. \tag{41}$$

Case V: If $\psi_0=\frac{\psi_1^2}{4\psi_2}$, $\psi_1>0$ *and* $\psi_2>0$ and $G_1^2-G_2^2>0$, we have

$$\mathcal{L}_{31}(x,t)=\frac{i\sqrt{2}\sqrt{\psi_2}\mu\mathrm{ck}\left(\pm\frac{\sqrt{-\frac{\psi_1}{\psi_2}}}{\sqrt{2}}\right)\tan\left(\frac{\sqrt{\psi_1}(\mathfrak{O}+\eta)}{\sqrt{2}}\right)}{\sqrt{\epsilon\mathrm{k}}}, \tag{42}$$

$$\mathcal{L}_{32}(x,t)=\frac{i\sqrt{2}\sqrt{\psi_2}\mu\mathrm{ck}\left(\pm\frac{\sqrt{-\frac{\psi_1}{\psi_2}}}{\sqrt{2}}\right)\cot\left(\frac{\sqrt{\psi_1}(\mathfrak{O}+\eta)}{\sqrt{2}}\right)}{\sqrt{\epsilon\mathrm{k}}}, \tag{43}$$

$$\mathcal{L}_{33}(x,t)=\frac{i\sqrt{2}\sqrt{\psi_2}\mu\mathrm{ck}\left(\pm\frac{\sqrt{\frac{\psi_1}{\psi_2}}}{\sqrt{2}}\right)\left(\tan\left(\sqrt{2}\sqrt{\psi_1}(\mathfrak{O}+\eta)\right)+\sec\left(\sqrt{2}\sqrt{\psi_1}(\mathfrak{O}+\eta)\right)\right)}{\sqrt{\epsilon\mathrm{k}}}, \tag{44}$$

$$\mathcal{L}_{34}(x,t)=\frac{i\sqrt{2}\sqrt{\psi_2}\mu\mathrm{ck}\left(\pm\frac{\sqrt{\frac{\psi_1}{\psi_2}}}{2\sqrt{2}}\right)\left(\tan\left(\frac{\sqrt{\psi_1}(\mathfrak{O}+\eta)}{2\sqrt{2}}\right)-\cot\left(\frac{\sqrt{\psi_1}(\mathfrak{O}+\eta)}{2\sqrt{2}}\right)\right)}{\sqrt{\epsilon\mathrm{k}}}, \tag{45}$$

$$\mathcal{L}_{35}(x,t)=\frac{i\sqrt{2}\sqrt{\psi_2}\mu\mathrm{ck}\left(\pm\frac{\sqrt{\frac{\psi_1}{\psi_2}}}{\sqrt{2}}\right)\left(\sqrt{G_1^2-G_2^2}-e_1\cos\left(\sqrt{2}\sqrt{\psi_1}(\mathfrak{O}+\eta)\right)\right)}{\sqrt{\epsilon\mathrm{k}}\left(G_2+e_1\sin\left(\sqrt{2}\sqrt{\psi_1}(\mathfrak{O}+\eta)\right)\right)}, \tag{46}$$

$$\mathcal{L}_{36}(x,t)=\frac{i\sqrt{2}\sqrt{\psi_2}\mu\mathrm{ck}\left(\pm\frac{\sqrt{\frac{\psi_1}{\psi_2}}}{\sqrt{2}}\right)\cos\left(\sqrt{2}\sqrt{\psi_1}(\mathfrak{O}+\eta)\right)}{\sqrt{\epsilon\mathrm{k}}\left(\sin\left(\sqrt{2}\sqrt{\psi_1}(\mathfrak{O}+\eta)\right)-1\right)}. \tag{47}$$

Case VI: If $\psi_0=0,\ \psi_1>0$, we have

$$\mathcal{L}_{37}(x,t)=\frac{i\sqrt{2}\sqrt{\psi_2}\mu\mathrm{ck}\left(\pm\frac{4\psi_1 e^{\sqrt{\psi_1}(\mathfrak{O}+\eta)}}{e^{2\sqrt{\psi_1}(\mathfrak{O}+\eta)}-4\psi_1\psi_2}\right)}{\sqrt{\epsilon\mathrm{k}}}, \tag{48}$$

$$\mathcal{L}_{38}(x,t)=\frac{i\sqrt{2}\sqrt{\psi_2}\mu\mathrm{ck}\left(\pm\frac{4\psi_1 e^{\sqrt{\psi_1}(\mathfrak{O}+\eta)}}{1-4\psi_1\psi_2 e^{2\sqrt{\psi_1}(\mathfrak{O}+\eta)}}\right)}{\sqrt{\epsilon\mathrm{k}}}. \tag{49}$$

Case VII: If $\psi_0=0,\ \psi_1=0$ *and* $\psi_2>0$, we have

$$\mathcal{L}_{39}(x,t)=\frac{i\sqrt{2}\sqrt{\psi_2}\mu\mathrm{ck}\left(\pm\frac{1}{\sqrt{\psi_2}(\mathfrak{O}+\eta)}\right)}{\sqrt{\epsilon\mathrm{k}}}, \tag{50}$$

$$\mathcal{L}_{40}(x,t) = \frac{i\sqrt{2}\sqrt{\psi_2}\mu \mathrm{ck}\left(\pm\frac{i}{\sqrt{\psi_2}(\mathfrak{V}+\eta)}\right)}{\sqrt{\epsilon \mathrm{k}}}, \tag{51}$$

where $\mathfrak{V} = \frac{k}{(\alpha+1)\Pi}x^{\alpha} - \frac{c}{(\alpha+1)\Pi}t^{\alpha} - x_0$.

5.2 Applications of the polynomial expansion technique

g'' and g^3 are balanced in Eq. (10), which results in $N = 1$. When $N = 1$, the solution to Eq. (7) accepts the form

$$\mathcal{L}(\mathfrak{V}) = m_0 + m_1\psi(\mathfrak{V}) + n_1\frac{1}{\psi(\mathfrak{V})}, \tag{52}$$

the following classes of solutions can be obtained by plugging Eq. (52), its second derivative, together with Eq. (8), into Eq. (10).

$$\begin{aligned}
6m_1m_0n_1\epsilon \mathrm{k} - m_0c + m_1\nu\Pi\mu \mathrm{ck}^2 + m_0^3\epsilon \mathrm{k} + n_1\nu\mu \mathrm{ck}^2 &= 0,\\
2n_1\Pi^2\mu \mathrm{ck}^2 + n_1^3\epsilon \mathrm{k} &= 0,\\
3m_0n_1^2\epsilon \mathrm{k} + 3n_1\nu\Pi\mu \mathrm{ck}^2 &= 0,\\
3m_1n_1^2\epsilon \mathrm{k} + 3m_0^2n_1\epsilon \mathrm{k} - n_1c + n_1\nu^2\mu \mathrm{ck}^2 + 2n_1\Pi\mu \mathrm{ck}^2 &= 0,\\
3m_1^2n_1\epsilon \mathrm{k} - m_1c + m_1\nu^2\mu \mathrm{ck}^2 + 2m_1\Pi\mu \mathrm{ck}^2 + 3m_0^2a_1\epsilon \mathrm{k} &= 0,\\
3m_1\nu\mu \mathrm{ck}^2 + 3m_0m_1^2\epsilon \mathrm{k} &= 0,\\
m_1^3\epsilon \mathrm{k} + 2m_1\mu \mathrm{ck}^2 &= 0.
\end{aligned}$$

The algebraic set of problems described above can be resolved using the Mathematica.

Family I:

$$a_0 = -\frac{\sqrt{c-2\Pi\mu \mathrm{ck}^2}}{\sqrt{\epsilon \mathrm{k}}},\ a_1 = 0,\ b_1 = -\frac{\sqrt{2}\Pi\mu \mathrm{ck}\sqrt{2\Pi\mu \mathrm{ck}^2-c}}{\sqrt{\epsilon \mathrm{k}}\sqrt{c-2\Pi\mu \mathrm{ck}^2}},\ \nu = -\frac{\sqrt{2}\sqrt{2\Pi\mu \mathrm{ck}^2-c}}{\mu \mathrm{ck}}.$$

When we input the mentioned results into Eq. (52), distinct sets of solutions for traveling waves are generated.

Case I.

$$\mathcal{L}_{41}(x,t) = \frac{\sqrt{2}\mathfrak{V}\Pi\mu \mathrm{ck}\sqrt{2\Pi\mu \mathrm{ck}^2-c}}{\sqrt{\epsilon \mathrm{k}}\sqrt{c-2\Pi\mu \mathrm{ck}^2}} - \frac{\sqrt{c-2\Pi\mu \mathrm{ck}^2}}{\sqrt{\epsilon \mathrm{k}}}. \tag{53}$$

Case II.

$$\mathcal{L}_{42}(x,t) = \frac{\sqrt{2}\mu \mathrm{ck}\sqrt{2\Pi\mu \mathrm{ck}^2-c}\left(K_0e^{-\mathfrak{V}\Pi}-1\right)}{\sqrt{\epsilon \mathrm{k}}\sqrt{c-2\Pi\mu \mathrm{ck}^2}} - \frac{\sqrt{c-2\Pi\mu \mathrm{ck}^2}}{\sqrt{\epsilon \mathrm{k}}}. \tag{54}$$

Case III.

$$\mathcal{L}_{43}(x,t) = -\frac{\sqrt{2}\sqrt{\Pi}\mu\mathrm{ck}\sqrt{2\Pi\mu\mathrm{ck}^2 - c}\cot\left(\mathfrak{O}\sqrt{\Pi}\right)}{\sqrt{\epsilon\mathrm{k}}\sqrt{c - 2\Pi\mu\mathrm{ck}^2}} - \frac{\sqrt{c - 2\Pi\mu\mathrm{ck}^2}}{\sqrt{\epsilon\mathrm{k}}}, \tag{55}$$

$$\mathcal{L}_{44}(x,t) = \frac{\sqrt{2}\Pi\mu\mathrm{ck}\sqrt{2\Pi\mu\mathrm{ck}^2 - c}\tan\left(\mathfrak{O}\sqrt{\Pi}\right)}{\sqrt{-\Pi}\sqrt{\epsilon\mathrm{k}}\sqrt{c - 2\Pi\mu\mathrm{ck}^2}} - \frac{\sqrt{c - 2\Pi\mu\mathrm{ck}^2}}{\sqrt{\epsilon\mathrm{k}}}. \tag{56}$$

Case IV.

$$\mathcal{L}_{45}(x,t) = \frac{\sqrt{2}\Pi\mu\mathrm{ck}\sqrt{2\Pi\mu\mathrm{ck}^2 - c}\coth\left(\mathfrak{O}\sqrt{-\Pi}\right)}{\sqrt{-\Pi}\sqrt{\epsilon\mathrm{k}}\sqrt{c - 2\Pi\mu\mathrm{ck}^2}} - \frac{\sqrt{c - 2\Pi\mu\mathrm{ck}^2}}{\sqrt{\epsilon\mathrm{k}}}, \tag{57}$$

$$\mathcal{L}_{46}(x,t) = -\frac{\sqrt{2}\Pi\mu\mathrm{ck}\sqrt{2\Pi\mu\mathrm{ck}^2 - c}\tanh\left(\mathfrak{O}\sqrt{-\Pi}\right)}{\sqrt{-\Pi}\sqrt{\epsilon\mathrm{k}}\sqrt{c - 2\Pi\mu\mathrm{ck}^2}} - \frac{\sqrt{c - 2\Pi\mu\mathrm{ck}^2}}{\sqrt{\epsilon\mathrm{k}}}. \tag{58}$$

Case V.

$$\mathcal{L}_{47}(x,t) = -\frac{\sqrt{2}\Pi\mu\mathrm{ck}\sqrt{2\Pi\mu\mathrm{ck}^2 - c}\left(1 - K_1 e^{\mathfrak{O}(\varrho_1 - \varrho_2)}\right)}{\sqrt{\epsilon\mathrm{k}}\sqrt{c - 2\Pi\mu\mathrm{ck}^2}\left(\varrho_1 - K_1\varrho_2 e^{\mathfrak{O}(\varrho_1 - \varrho_2)}\right)} - \frac{\sqrt{c - 2\Pi\mu\mathrm{ck}^2}}{\sqrt{\epsilon\mathrm{k}}}, \tag{59}$$

where $\mathfrak{O} = \frac{k}{(\alpha+1)\Pi}x^{\alpha} - \frac{c}{(\alpha+1)\Pi}t^{\alpha} - x_0$.

Family II:

The results for the second category are provided below,

$$a_0 = -\frac{\sqrt{c - 2\Pi\mu\mathrm{ck}^2}}{\sqrt{\epsilon\mathrm{k}}},\ a_1 = 0,\ b_1 = \frac{\sqrt{2}\Pi\mu\mathrm{ck}\sqrt{2\Pi\mu\mathrm{ck}^2 - c}}{\sqrt{\epsilon\mathrm{k}}\sqrt{c - 2\Pi\mu\mathrm{ck}^2}},\ \nu = \frac{\sqrt{2}\sqrt{2\Pi\mu\mathrm{ck}^2 - c}}{\mu\mathrm{ck}}.$$

When we input the mentioned results into Eq. (52), distinct sets of solutions for traveling waves are generated.

Case I.

$$\mathcal{L}_{48}(x,t) = -\frac{\sqrt{2}\mathfrak{O}\Pi\mu\mathrm{ck}\sqrt{2\Pi\mu\mathrm{ck}^2 - c}}{\sqrt{\epsilon\mathrm{k}}\sqrt{c - 2\Pi\mu\mathrm{ck}^2}} - \frac{\sqrt{c - 2\Pi\mu\mathrm{ck}^2}}{\sqrt{\epsilon\mathrm{k}}}. \tag{60}$$

Case II.

$$\mathcal{L}_{49}(x,t) = -\frac{\sqrt{2}\mu\mathrm{ck}\sqrt{2\Pi\mu\mathrm{ck}^2 - c}\left(K_0 e^{-\mathfrak{O}\Pi} - 1\right)}{\sqrt{\epsilon\mathrm{k}}\sqrt{c - 2\Pi\mu\mathrm{ck}^2}} - \frac{\sqrt{c - 2\Pi\mu\mathrm{ck}^2}}{\sqrt{\epsilon\mathrm{k}}}. \tag{61}$$

Case III.

$$\mathcal{L}_{50}(x,t) = \frac{\sqrt{2}\sqrt{\Pi}\mu\mathrm{ck}\sqrt{2\Pi\mu\mathrm{ck}^2 - c}\cot\left(\mho\sqrt{\Pi}\right)}{\sqrt{\epsilon\mathrm{k}}\sqrt{c - 2\Pi\mu\mathrm{ck}^2}} - \frac{\sqrt{c - 2\Pi\mu\mathrm{ck}^2}}{\sqrt{\epsilon\mathrm{k}}}, \tag{62}$$

$$\mathcal{L}_{51}(x,t) = -\frac{\sqrt{2}\Pi\mu\mathrm{ck}\sqrt{2\Pi\mu\mathrm{ck}^2 - c}\tan\left(\mho\sqrt{\Pi}\right)}{\sqrt{-\Pi}\sqrt{\epsilon\mathrm{k}}\sqrt{c - 2\Pi\mu\mathrm{ck}^2}} - \frac{\sqrt{c - 2\Pi\mu\mathrm{ck}^2}}{\sqrt{\epsilon\mathrm{k}}}. \tag{63}$$

Case IV.

$$\mathcal{L}_{52}(x,t) = -\frac{\sqrt{2}\Pi\mu\mathrm{ck}\sqrt{2\Pi\mu\mathrm{ck}^2 - c}\coth\left(\mho\sqrt{-\Pi}\right)}{\sqrt{-\Pi}\sqrt{\epsilon\mathrm{k}}\sqrt{c - 2\Pi\mu\mathrm{ck}^2}} - \frac{\sqrt{c - 2\Pi\mu\mathrm{ck}^2}}{\sqrt{\epsilon\mathrm{k}}}, \tag{64}$$

$$\mathcal{L}_{53}(x,t) = \frac{\sqrt{2}\Pi\mu\mathrm{ck}\sqrt{2\Pi\mu\mathrm{ck}^2 - c}\tanh\left(\mho\sqrt{-\Pi}\right)}{\sqrt{-\Pi}\sqrt{\epsilon\mathrm{k}}\sqrt{c - 2\Pi\mu\mathrm{ck}^2}} - \frac{\sqrt{c - 2\Pi\mu\mathrm{ck}^2}}{\sqrt{\epsilon\mathrm{k}}}. \tag{65}$$

Case V.

$$\mathcal{L}_{54}(x,t) = \frac{\sqrt{2}\Pi\mu\mathrm{ck}\sqrt{2\Pi\mu\mathrm{ck}^2 - c}\left(1 - K_1 e^{\mho(\varrho_1 - \varrho_2)}\right)}{\sqrt{\epsilon\mathrm{k}}\sqrt{c - 2\Pi\mu\mathrm{ck}^2}\left(\varrho_1 - K_1\varrho_2 e^{\mho(\varrho_1 - \varrho_2)}\right)} - \frac{\sqrt{c - 2\Pi\mu\mathrm{ck}^2}}{\sqrt{\epsilon\mathrm{k}}}, \tag{66}$$

where $\mho = \frac{k}{(\alpha+1)\Pi}x^{\alpha} - \frac{c}{(\alpha+1)\Pi}t^{\alpha} - x_0$.

6 Stability analysis

In Eq. (1), we establish the Hamiltonian and momentum for the described strategy, providing a clear definition for these parameters (Alhefthi et al. 2024; Rizvi et al. 2024)

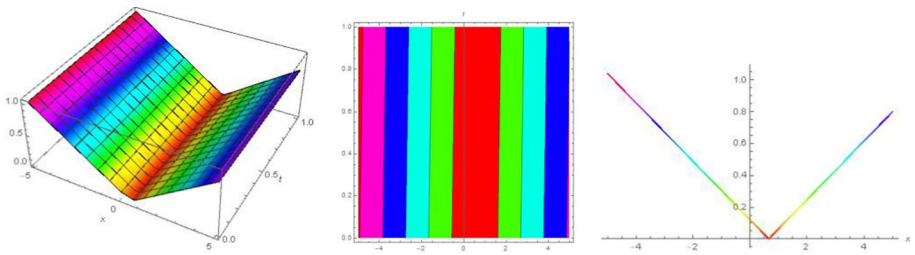

(a) (b) (c)

Fig. 1 **a** Represents 3D plot of a v-shaped dark soliton in x, t and $\mathcal{L}(x,t)$ dimensions. In **b**, there's a contour plot offering a different view, while **c** simplifies the depiction with a 2D plot of the solution for $\mathcal{L}_1(x,t)$ highlighting specific values $\alpha = 1$, $c = 1.2$, $\Gamma = 1.22$, $\eta = 1$, $k = 1.1$, $x_0 = 1.23$, $y_1 = 0.11$, $y_2 = 0.5$, $\epsilon = 1$, $\mu = 1$

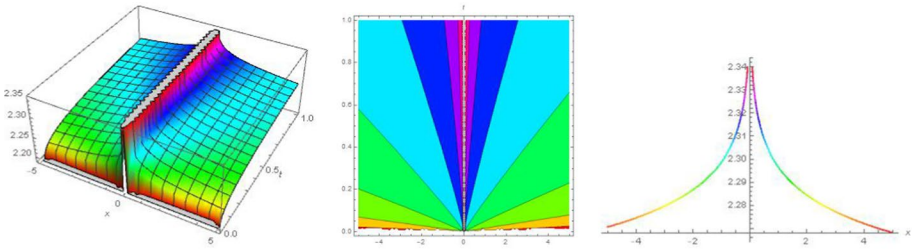

(a) (b) (c)

Fig. 2 **a** Represents the solution 3D plot of a bell shaped singular soliton in x, t and $\mathcal{L}(x,t)$ dimensions. In **b**, there's a contour plot offering a different view, while **c** simplifies the depiction with a 2D plot of the solution for $\mathcal{L}_2(x,t)$ highlighting specific values $y_1 = 1,\ y_2 = 1.5,\ \mu = 1,\ c = 1.02,\ k = 1.1,\ \eta = -1,\ x_0 = 1.23,\ \alpha = 0.02,\ \Gamma = 1.22,\ \epsilon = 1$

$$S = \frac{1}{2}\int_{-\infty}^{\infty} \mathcal{H}^2\, d\psi, \tag{67}$$

the electrical potential, denoted by $\mathcal{H}$, and momentum represented by S, are key elements for stabilizing solitary waves is

$$\frac{\partial S}{\partial \sigma} > 0, \tag{68}$$

Therefore, σ represents frequency. We derive Eq. (67), incorporating the traveling wave solution from Eq. (15)

$$S = \frac{1}{2}\int_{-10}^{10} \left(-\frac{ic\sqrt{-\frac{y_1}{y_2}}\sqrt{y_2}\mu \tanh\left(\frac{\sqrt{-y_1}\left(-cy_1\mu+\eta+\frac{x}{2}-1\right)}{\sqrt{2}}\right)}{\sqrt{\epsilon}} \right)^2 dx, \tag{69}$$

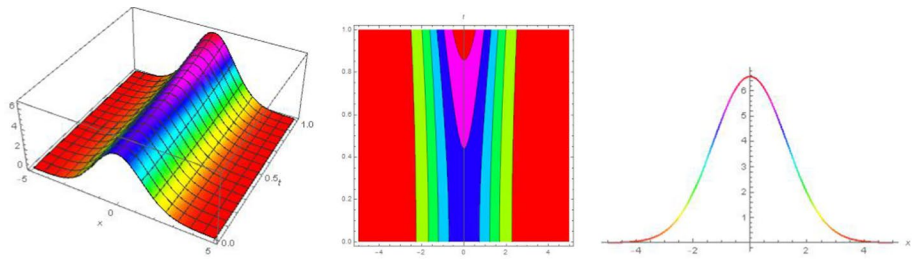

(a) (b) (c)

Fig. 3 **a** Represents the solution 3D plot of a bell shaped bright soliton in x, t and $\mathcal{L}(x,t)$ dimensions. In **b**, there's a contour plot offering a different view, while **c** simplifies the depiction with a 2D plot of the solution for $\mathcal{L}_3(x,t)$ highlighting specific values $y_1 = 1,\ y_2 = 4f_1f_2,\ \mu = 1,\ c = 1.02,\ k = 1.1,\ \eta = 0.1,\ f_1 = -1,\ f_2 = 1,\ x_0 = 1.23,\ \alpha = 2,\ \Gamma = 1.22,\ \epsilon = 1$

after simplification, we obtain

$$S = \frac{c^2\sqrt{y_1}\mu^2\left(10\sqrt{y_1} - \sqrt{2}\left(\tan\left(\frac{\sqrt{y_1}(cy_1\mu-\eta+6)}{\sqrt{2}}\right) + \tan\left(\frac{\sqrt{y_1}(-cy_1\mu+\eta+4)}{\sqrt{2}}\right)\right)\right)}{\epsilon}. \quad (70)$$

Applying the stabilization condition for solitary waves, we conclude that a stable nonlinear model is represented by Eq. (1).

7 Physical description of the solutions

We discuss about how the space-time fractional MEW equation's conclusions should be interpreted physically. The solutions obtained here include those for soliton waves, bright and dark solitons, multi-solitons, periodic solitary waves, rational functions, and elliptic functions for certain relevant parameter values. In this research, we have applied two innovative methods namely the polynomial expansion approach and the Sardar sub-equation method to the space-time fractional MEWE. These methods, which have not been previously employed for this equation, offer new insights and analytical solutions that contribute to the broader understanding of fractional PDEs. The nature of nonlinear waves created from Eq. (1) is visualised in the 3D, contour and 2D graphs. Figures display the graphical representations of some of the solutions that were obtained. Below are the physical explanations for these figures.

Figure 1 show how dark soliton solutions emerge under specific parameter values $\alpha = 1,\ c = 1.2,\ \Gamma = 1.22,\ \eta = 1,\ k = 1.1,\ x_0 = 1.23,\ y_1 = 0.11,\ y_2 = 0.5,\ \epsilon = 1,\ \mu = 1$. In Figs. 2, 7, 9, 10 the solution's behavior is represented by a distinct bell-shaped pattern, influenced by specific parameters $y_1 = 1,\ y_2 = 1.5,\ \mu = 1,\ c = 1.02,\ k = 1.1,\ \eta = -1,\ x_0 = 1.23,\ \alpha = 0.02,\ \Gamma = 1.22,\ \epsilon = 1$ and $\omega = 2,\ \nu = 0.001,\ \mu = 1,\ c = 2,\ k = 2,\ \Omega = -2,\ x_0 = 1.02,\ \Gamma = 1,\ \alpha = 1.3,\ \epsilon = 1$ and $\omega = 1,\ \nu = 0.001,\ \mu = 1,\ c = -1,\ k = 2,\ \Pi = -1,\ x_0 = 1.02,\ \Gamma = 1,\ \alpha = 1.3,\ \epsilon = 1$. For the set of appropriate values $y_1 = 1,\ y_2 = 4f_1f_2,\ \mu = 1,\ c = 1.02,\ k = 1.1,\ \eta = 0.1,\ f_1 = -1,\ f_2 = 1,\ x_0 = 1.23,\ \alpha = 2,\ \Gamma = 1.22,\ \epsilon = 1$, bright typed soliton is represented in Fig. 3, whereas Fig. 5 produces a W-shaped solution for different constant values $y_1 = -1,\ y_2 = 1,\ y_0 = \frac{y_1^2}{4y_2},\ \mu = 1,\ c = 1.02,\ k = 1.1,\ \eta = -1,$

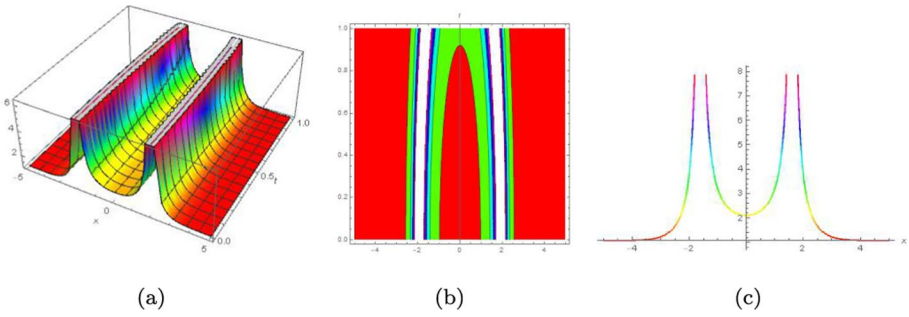

(a) (b) (c)

Fig. 4 **a** Represents the solution 3D plot of a double peaked singular soliton in x, t and $\mathcal{L}(x,t)$ dimensions. In **b**, there's a contour plot offering a different view, while **c** simplifies the depiction with a 2D plot of the solution for $\mathcal{L}_4(x,t)$ highlighting specific values $y_1 = -1,\ y_2 = 1,\ y_0 = \frac{y_1^2}{4y_2},\ \mu = 1,\ c = 1.02,\ k = 1.1,$ $\eta = 0.1,\ f_1 = -1,\ f_2 = 1,\ x_0 = 1.23,\ \alpha = 2,\ \Gamma = 1.22,\ \epsilon = 1$

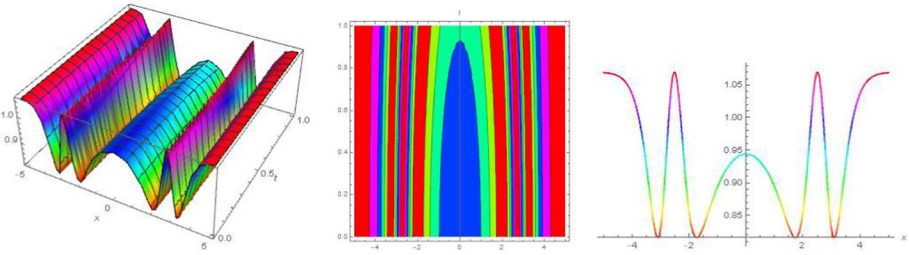

(a) (b) (c)

Fig. 5 **a** Represents the solution 3D plot of a multiple peaked bright soliton in x, t and $\mathcal{L}(x,t)$ dimensions. In **b**, there's a contour plot offering a different view, while **c** simplifies the depiction with a 2D plot of the solution for $\mathcal{L}_5(x,t)$ highlighting specific values $y_1 = -1,\ y_2 = 1,\ y_0 = \frac{y_1^2}{4y_2},\ \mu = 1,\ c = 1.02,\ k = 1.1,\ \eta = -1,\ f_1 = 0.1,\ f_2 = 1,\ x_0 = 1.23,\ \alpha = 2,\ \Gamma = 1.22,\ \epsilon = 1$

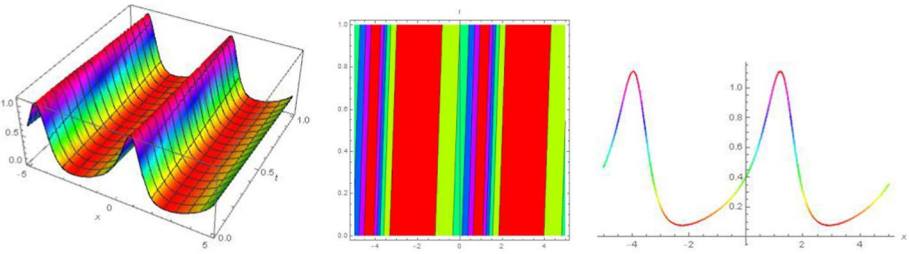

(a) (b) (c)

Fig. 6 **a** Represents the solution 3D plot of a μ shaped bright soliton in x, t and $\mathcal{L}(x,t)$ dimensions. In **b**, there's a contour plot offering a different view, while **c** simplifies the depiction with a 2D plot of the solution for $\mathcal{L}_{15}(x,t)$ highlighting specific values $y_1 = 1, \}y_2 = 2,\ y_0 = \frac{y_1^2}{4y_2},\ G_1 = 3,\ G_2 = 2,\ \mu = 0.1,\ c = 1.6,\ k = 2.1,\ \eta = -1,\ x_0 = 1,\ \alpha = 1,\ \Gamma = 1.22,\ \epsilon = 1,\ e_1 = 1.5$

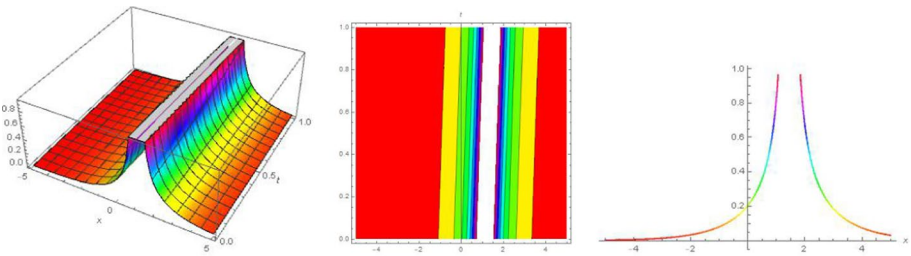

(a) (b) (c)

Fig. 7 **a** Represents the solution 3D plot of a bright singular soliton in x, t and $\mathcal{L}(x,t)$ dimensions. In **b**, there's a contour plot offering a different view, while **c** simplifies the depiction with a 2D plot of the solution for $\mathcal{L}_{18}(x,t)$ highlighting specific values $y_1 = 1,\ y_2 = 2,\ y_0 = \frac{y_1^2}{4y_2},\ \mu = 0.1,\ c = 1.6,\ k = 2.1,\ \eta = -1,\ x_0 = 1,\ \alpha = 1,\ \Gamma = 1.22,\ \epsilon = 1$

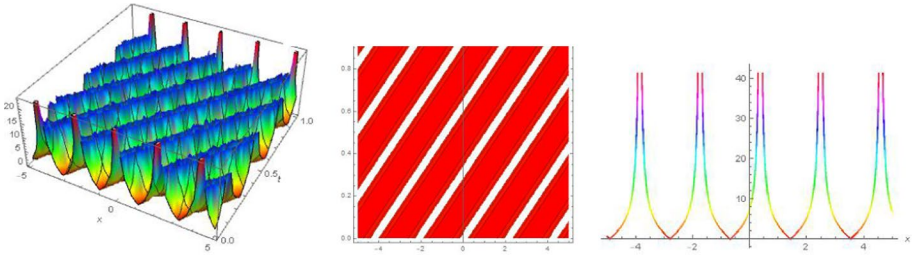

(a) (b) (c)

Fig. 8 **a** Represents the solution 3D plot of a v-shaped singular periodic soliton in x, t and $\mathcal{L}(x,t)$ dimensions. In **b**, there's a contour plot offering a different view, while **c** simplifies the depiction with a 2D plot of the solution for $\mathcal{L}_{34}(x,t)$ highlighting specific values $y_1 = 1,\ y_2 = 2,\ \mu = 2,\ c = 1.6,\ k = 2.1,\ \eta = 2,\ x_0 = 2,\ \alpha = 1,\ \Gamma = 0.5,\ \epsilon = 1$

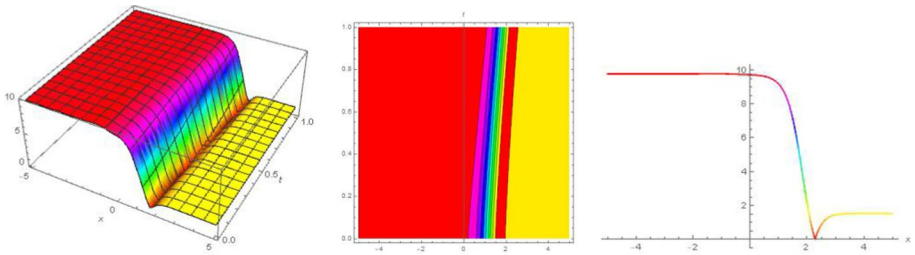

(a) (b) (c)

Fig. 9 **a** Represents the solution 3D plot of a solitary wave soliton in x, t and $\mathcal{L}(x,t)$ dimensions. In **b**, there's a contour plot offering a different view, while **c** simplifies the depiction with a 2D plot of the solution for $\mathcal{L}_{44}(x,t)$ highlighting specific values $\omega = 2,\ \nu = 0.001,\ \mu = 1,\ c = 2,\ k = 2,\ \Pi = -2,\ x_0 = 1.02,\ \Gamma = 1,\ \alpha = 1.3,\ \epsilon = 1$

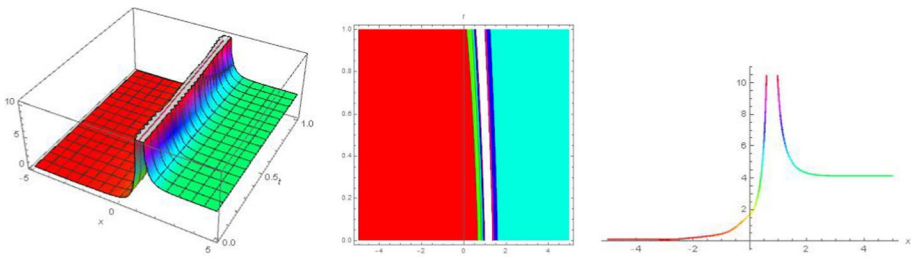

(a) (b) (c)

Fig. 10 **a** represents the solution 3D plot of a singular bright soliton in x, t and $\mathcal{L}(x,t)$ dimensions. In **b**, there's a contour plot offering a different view, while **c** simplifies the depiction with a 2D plot of the solution for $\mathcal{L}_{45}(x,t)$ highlighting specific values $\omega = 1,\ \nu = 0.001,\ \mu = 1,\ c = -1,\ k = 2,\ \Pi = -1,\ x_0 = 1.02,\ \Gamma = 1,\ \alpha = 1.3,\ \epsilon = 1$

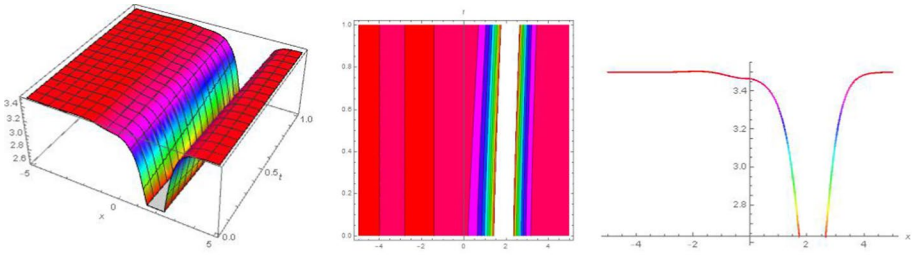

Fig. 11 **a** Represents the solution 3D plot of a dark singular soliton in x, t and $\mathcal{L}(x,t)$ dimensions. In **b**, there's a contour plot offering a different view, while **c** simplifies the depiction with a 2D plot of the solution for $\mathcal{L}_{46}(x,t)$ highlighting specific values $\omega = 3.3,\ \nu = 0.001,\ \mu = 2,\ c = 1,\ k = 2,\ \Pi = -1,\ x_0 = 2,\ \Gamma = 1,\ \alpha = 1.3,\ \epsilon = 2$

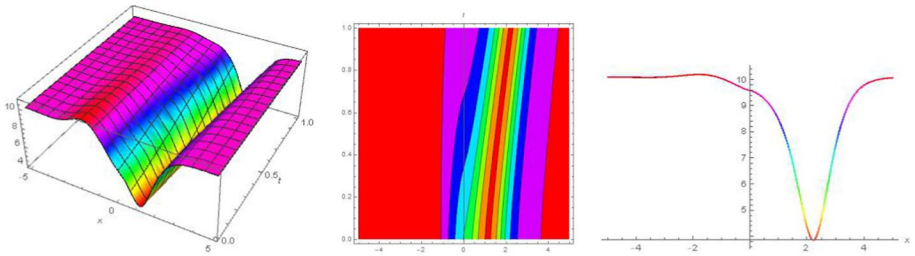

Fig. 12 **a** Represents the solution 3D plot of a bell shaped dark soliton in x, t and $\mathcal{L}(x,t)$ dimensions. In **b**, there's a contour plot offering a different view, while **c** simplifies the depiction with a 2D plot of the solution for $\mathcal{L}_{53}(x,t)$ highlighting specific values $\omega = 1,\ \nu = 0.001,\ \mu = 2,\ c = 3.3,\ k = 2,\ \Pi = -0.5,\ x_0 = 1.02,\ \Gamma = 1,\ \alpha = 1.3,\ \epsilon = 1$

$f_1 = 0.1,\ f_2 = 1,\ x_0 = 1.23,\ \alpha = 2,\ \Gamma = 1.22,\ \epsilon = 1$. For the set of appropriate values $y_1 = 1,\ y_2 = 2,\ \mu = 2,\ c = 1.6,\ k = 2.1,\ \eta = 2,\ x_0 = 2,\ \alpha = 1,\ \Gamma = 0.5,\ \epsilon = 1$, the parabolic wave solution is represented in Fig. 8. Furthermore, for different constant values $\omega = 3.3,\ \nu = 0.001,\ \mu = 2,\ c = 1,\ k = 2,\ \Pi = -1,\ x_0 = 2,\ \Gamma = 1,\ \alpha = 1.3,\ \epsilon = 2$ and $\omega = 1,\ \nu = 0.001,\ \mu = 2,\ c = 3.3\ , k = 2,\ \Pi = -0.5,\ x_0 = 1.02,\ \Gamma = 1,\ \alpha = 1.3,\ \epsilon = 1$, represents dark type structure soliton solutions are shown in Figs. 11, 12.

8 Conclusion

In the context of the ongoing research, the modified Sardar sub-equation approach and the polynomial expansion method were used in this study to provide exact solutions for the conformable space-time fractional MEW problem, encompassing bright and dark soliton, periodic solitons and various other solution types. The Sardar sub-equation method is generally more effective due to its accuracy, stability, efficiency, simplicity, and versatility. However, the polynomial expansion approach can still be valuable for specific types of solutions where it excels in accuracy. Employing two distinct methodologies, we were

able to directly and effectively acquire these solutions, contributing to a comprehensive understanding of the behavior and dynamics described by the fractional differential equations. Studying fractional nonlinear problems is essential for enhancing our understanding and modeling of complex systems, improving predictive capabilities, and developing new mathematical tools and techniques. The article presents new solutions to the nonlinear evolution equation by employing these techniques. With the help of the Mathematica software, every calculation in this work has been performed and verified by back substitution (Figs. 3, 4, 5, 6, 7, 8, 9, 10, 11, 12).

Acknowledgements The authors would like to extend their sincere appreciations the Hubei University of Automotive Technology, P. R. China in the form of a start-up research Grant (BK202212). The authors extend their appreciation to Taif University, Saudi Arabia, for supporting this work through project number (TU-DSPP-2024-106).

Author Contributions Fazal Badshah: Software, scientific computation, review and editing. Kalim U. Tariq: Methodology, conceptualization, resource, validation. Mustafa Inc: Supervision, project administration. Shahram Rezapour: writing original draft, visualization, resources. A.S.A. Alsubaie: Software, resources. Sana Nisar: Formal analysis and investigation, writing original draft, visualization.

Funding Open access funding provided by the Scientific and Technological Research Council of Türkiye (TÜBİTAK). The authors extend their appreciation to Taif University, Saudi Arabia, for supporting this work through project number (TU-DSPP-2024-106).

Availability of data and materials As this study did not entail the analysis of specific datasets, data sharing is deemed not applicable to this article.

Declarations

Conflict of interest The authors assert that they do not have any identifiable conflicting financial interests or personal relationships that could be perceived as influencing the findings reported in this paper.

Ethical approval Not applicable.

Open Access This article is licensed under a Creative Commons Attribution 4.0 International License, which permits use, sharing, adaptation, distribution and reproduction in any medium or format, as long as you give appropriate credit to the original author(s) and the source, provide a link to the Creative Commons licence, and indicate if changes were made. The images or other third party material in this article are included in the article's Creative Commons licence, unless indicated otherwise in a credit line to the material. If material is not included in the article's Creative Commons licence and your intended use is not permitted by statutory regulation or exceeds the permitted use, you will need to obtain permission directly from the copyright holder. To view a copy of this licence, visit http://creativecommons.org/licenses/by/4.0/.

References

Abdel-Aty, A.-H., Kadry, H., Zidan, M., Al-Sbou, Y., Zanaty, E., Abdel-Aty, M.: A quantum classification algorithm for classification incomplete patterns based on entanglement measure. J. Intell. Fuzzy Syst. **38**(3), 2809–2816 (2020)

Alhefthi, R.K., Tariq, K.U., Wazwaz, A.-M., Mehboob, F.: On the nonlinear wave structures and stability analysis for the new generalized stochastic fractional potential-KDV model in dispersive medium. Opt. Quant. Electron. **56**(4), 662 (2024)

Ali, U., Ahmad, H., Baili, J., Botmart, T., Aldahlan, M.A.: Exact analytical wave solutions for space-time variable-order fractional modified equal width equation. Results Phys. **33**, 105216 (2022)

Almeida, R.: A Caputo fractional derivative of a function with respect to another function. Commun. Nonlinear Sci. Numer. Simul. **44**, 460–481 (2017)

Alquran, M.: New interesting optical solutions to the quadratic-cubic Schrodinger equation by using the Kudryashov-expansion method and the updated rational sine-cosine functions. Opt. Quant. Electron. **54**(10), 666 (2022)
Alquran, M.: Classification of single-wave and bi-wave motion through fourth-order equations generated from the ITO model. Phys. Scr. **98**(8), 085207 (2023)
Alquran, M., Al Smadi, T.: Generating new symmetric bi-peakon and singular bi-periodic profile solutions to the generalized doubly dispersive equation. Opt. Quant. Electron. **55**(8), 736 (2023)
Aminikhah, H., Sheikhani, A.R., Rezazadeh, H.: Exact solutions for the fractional differential equations by using the first integral method. Nonlinear Eng. **4**(1), 15–22 (2015)
Bashar, M.H., Arafat, S.Y., Islam, S.R., Rahman, M.M.: Wave solutions of the couple Drinfel'd–Sokolov–Wilson equation: new wave solutions and free parameters effect, J. Ocean Eng. Sci. (2022)
Bashar, M.H., Islam, S.R.: Exact solutions to the (2+ 1)-dimensional Heisenberg ferromagnetic spin chain equation by using modified simple equation and improve f-expansion methods. Phys. Open **5**, 100027 (2020)
Bekir, A., Shehata, M.S., Zahran, E.H.: New perception of the exact solutions of the 3d-fractional Wazwaz–Benjamin–Bona–Mahony (3D-FWBBM) equation. J. Interdiscip. Math. **24**(4), 867–880 (2021)
Chen, C., Jiang, Y.-L.: Simplest equation method for some time-fractional partial differential equations with conformable derivative. Comput. Math. Appl. **75**(8), 2978–2988 (2018)
Demirbilek, U., Mamedov, K.R.: Application of ibsef method to chaffee-infante equation in (1+ 1) and (2+ 1) dimensions. Comput. Math. Math. Phys. **63**(8), 1444–1451 (2023)
Gurefe, Y.: The generalized Kudryashov method for the nonlinear fractional partial differential equations with the beta-derivative. Revista Mexicana de Física **66**(6), 771–781 (2020)
Hosseini, K., Ayati, Z.: Exact solutions of space-time fractional ew and modified ew equations using Kudryashov method. Nonlinear Sci. Lett. A **7**(2), 58–66 (2016)
Ikram, M., Muhammad, A., Rahmn, A.U.: Analytic solution to Benjamin–Bona–Mahony equation by using Laplace Adomian decomposition method. Matrix Sci. Math. **3**(1), 01–04 (2019)
Jafari, H., Soltani, R., Masood Khalique, C., Baleanu, D.: On the exact solutions of nonlinear long-short wave resonance equations. Rom. Rep. Phys **67**(3), 762–772 (2015)
Jaradat, I., Alquran, M.: Construction of solitary two-wave solutions for a new two-mode version of the Zakharov–Kuznetsov equation. Mathematics **8**(7), 1127 (2020)
Jaradat, I., Alquran, M.: A variety of physical structures to the generalized equal-width equation derived from Wazwaz–Benjamin–Bona–Mahony model. J. Ocean Eng. Sci. **7**(3), 244–247 (2022)
Jena, R.M., Chakraverty, S.: Q-homotopy analysis aboodh transform method based solution of proportional delay time-fractional partial differential equations. J. Interdiscip. Math. **22**(6), 931–950 (2019)
Jumarie, G.: Modified Riemann–Liouville derivative and fractional Taylor series of nondifferentiable functions further results. Comput. Math. Appl. **51**(9–10), 1367–1376 (2006)
Kadkhoda, N., Jafari, H.: Analytical solutions of the Gerdjikov–Ivanov equation by using exp (- φ (ξ))-expansion method. Optik **139**, 72–76 (2017)
Khater, A., Callebaut, D., Seadawy, A.: General soliton solutions for nonlinear dispersive waves in convective type instabilities. Phys. Scr. **74**(3), 384 (2006)
Khodadad, F.S., Nazari, F., Eslami, M., Rezazadeh, H.: Soliton solutions of the conformable fractional Zakharov–Kuznetsov equation with dual-power law nonlinearity. Opt. Quant. Electron. **49**, 1–12 (2017)
Kırcı, Ö., Koç, D.A., Bulut, H.: Dynamics of the traveling wave solutions of conformable time-fractional ISLW and DJKM equations via a new expansion method. Opt. Quant. Electron. **56**(6), 933 (2024)
Korkmaz, A.: Exact solutions of space-time fractional ew and modified ew equations. Chaos Solitons Fract. **96**, 132–138 (2017)
Lu, D., Seadawy, A.R., Ali, A.: Applications of exact traveling wave solutions of modified Liouville and the symmetric regularized long wave equations via two new techniques. Results Phys. **9**, 1403–1410 (2018)
Ma, W.-X., Yong, X., Zhang, H.-Q.: Diversity of interaction solutions to the (2+ 1)-dimensional ITO equation. Comput. Math. Appl. **75**(1), 289–295 (2018)
Manafian, J., Lakestani, M.: A new analytical approach to solve some of the fractional-order partial differential equations. Indian J. Phys. **91**, 243–258 (2017)
Nawaz, B., Ali, K., Rizvi, S., Younis, M.: Soliton solutions for Quintic complex Ginzburg–Landau model. Superlattices Microstruct. **110**, 49–56 (2017)
Oldham, K., Spanier, J.: The Fractional Calculus Theory and Applications of Differentiation and Integration to Arbitrary Order. Elsevier, Amsterdam (1974)

Osman, M., Korkmaz, A., Rezazadeh, H., Mirzazadeh, M., Eslami, M., Zhou, Q.: The unified method for conformable time fractional Schrödinger equation with perturbation terms. Chin. J. Phys. **56**(5), 2500–2506 (2018)
Pandir, Y., Yasmin, H.: Optical soliton solutions of the generalized Sine-Gordon equation. Electron. J. Appl. Math. **1**(2), 71–86 (2023)
Podlubny, I.: An introduction to fractional derivatives, fractional differential equations, to methods of their solution and some of their applications. Math. Sci. Eng. **198**, 340 (1999)
Rafiq, M.N., Majeed, A., Inc, M., Kamran, M.: New traveling wave solutions for space-time fractional modified equal width equation with beta derivative. Phys. Lett. A **446**, 128281 (2022)
Raslan, K., El-Danaf, T.S., Ali, K.K.: Exact solution of the space-time fractional coupled ew and coupled mew equations. Eur. Phys. J. Plus **132**, 1–11 (2017)
Raslan, K., Ali, K.K., Shallal, M.A.: The modified extended tanh method with the Riccati equation for solving the space-time fractional ew and mew equations. Chaos Solitons Fract. **103**, 404–409 (2017)
Rasool, T., Hussain, R., Rezazadeh, H., Ali, A., Demirbilek, U.: Novel soliton structures of truncated m-fractional (4+ 1)-dim fokas wave model. Nonlinear Eng. **12**(1), 20220292 (2023)
Rezazadeh, H., Abazari, R., Khater, M.M., Inc, M., Baleanu, D.: New optical solitons of conformable resonant nonlinear schrödinger's equation. Open Phys. **18**(1), 761–769 (2020)
Rizvi, S.T.R., Ali, K., Aziz, N., Seadawy, A.R.: Lie symmetry analysis, conservation laws and soliton solutions by complete discrimination system for polynomial approach of landau Ginzburg Higgs equation along with its stability analysis, Optik 171675 (2024)
Sagheer, A., Zidan, M., Abdelsamea, M.M.: A novel autonomous perceptron model for pattern classification applications. Entropy **21**(8), 763 (2019)
Seadawy, A.R.: Three-dimensional weakly nonlinear shallow water waves regime and its traveling wave solutions. Int. J. Comput. Methods **15**(03), 1850017 (2018)
Seadawy, A.R., El-Rashidy, K.: Dispersive solitary wave solutions of Kadomtsev–Petviashvili and modified Kadomtsev–Petviashvili dynamical equations in unmagnetized dust plasma. Results Phys. **8**, 1216–1222 (2018)
Seadawy, A.R., Manafian, J.: New soliton solution to the longitudinal wave equation in a magneto-electro-elastic circular rod. Results Phys. **8**, 1158–1167 (2018)
Seadawy, A.R., Lu, D., Khater, M.M.: Solitary wave solutions for the generalized Zakharov–Kuznetsov–Benjamin–Bona–Mahony nonlinear evolution equation. J. Ocean Eng. Sci. **2**(2), 137–142 (2017)
Seadawy, A.R., Ali, A., Althobaiti, S., El-Rashidy, K.: Construction of abundant novel analytical solutions of the space-time fractional nonlinear generalized equal width model via riemann-liouville derivative with application of mathematical methods. Open Phys. **19**(1), 657–668 (2021)
Seadawy, A.R., Ali, A., Altalbe, A., Bekir, A.: Exact solutions of the (3+ 1)-generalized fractional nonlinear wave equation with gas bubbles. Sci. Rep. **14**(1), 1862 (2024)
Shallal, M.A., Ali, K.K., Raslan, K.R., Rezazadeh, H., Bekir, A.: Exact solutions of the conformable fractional ew and mew equations by a new generalized expansion method. J. Ocean Eng. Sci. **5**(3), 223–229 (2020)
Tajadodi, H., Khan, Z.A., Gómez-Aguilar, J., Khan, A., Khan, H., et al.: Exact solutions of conformable fractional differential equations. Results Phys. **22**, 103916 (2021)
Tariq, K.U., Seadawy, A.R., Younis, M., Rizvi, S.T.R.: Dispersive traveling wave solutions to the space-time fractional equal-width dynamical equation and its applications. Opt. Quant. Electron. **50**, 1–16 (2018)
Tariq, K.U., Inc, M., Hashemi, M.S.: On the soliton structures to the space-time fractional generalized reaction duffing model and its applications. Opt. Quant. Electron. **56**(4), 708 (2024)
Torvattanabun, M., Juntakud, P., Saiyun, A., Khansai, N.: The new exact solutions of the new coupled Konno–Oono equation by using extended simplest equation method. Appl. Math. Sci. **12**(6), 293–301 (2018)
Wu, G.-Z., Yu, L.-J., Wang, Y.-Y.: Fractional optical solitons of the space-time fractional nonlinear Schrödinger equation. Optik **207**, 164405 (2020)
Zafar, A.: Rational exponential solutions of conformable space-time fractional equal-width equations. Nonlinear Eng. **8**(1), 350–355 (2019)
Zaman, U., Arefin, M.A., Akbar, M.A., Uddin, M.H.: Solitary wave solution to the space-time fractional modified equal width equation in plasma and optical fiber systems. Results Phys. **52**, 106903 (2023)
Zidan, M., Abdel-Aty, A.-H., El-Sadek, A., Zanaty, E., Abdel-Aty, M.: Low-cost autonomous perceptron neural network inspired by quantum computation, in: AIP conference proceedings, Vol. 1905, AIP Publishing, (2017)
Zidan, M., Abdel-Aty, A.-H., El-shafei, M., Feraig, M., Al-Sbou, Y., Eleuch, H., Abdel-Aty, M.: Quantum classification algorithm based on competitive learning neural network and entanglement measure. Appl. Sci. **9**(7), 1277 (2019)

Authors and Affiliations

Fazal Badshah[1] · Kalim U. Tariq[2] · Mustafa Inc[3] · Shahram Rezapour[4] · Abdullah Saad Alsubaie[5] · Sana Nisar[2]

✉ Mustafa Inc
minc@firat.edu.tr

Kalim U. Tariq
kalimulhaq@must.edu.pk

Shahram Rezapour
rezapourshahram@yahoo.ca

[1] School of Electrical and Information Engineering, Hubei University of Automotive Technology, Shiyan 442002, People's Republic of China

[2] Department of Mathematics, Mirpur University of Science and Technology, Mirpur, AJK 10250, Pakistan

[3] Science Faculty, Department of Mathematics, Firat University, Elazig 23119, Turkey

[4] Department of Medical Research, China Medical University, Taichung 40402, Taiwan

[5] Department of Physics, College of Khurma University, Taif University, 21944 Taif, Saudi Arabia